HHS Public Access

Author manuscript

IEEE Trans Neural Syst Rehabil Eng. Author manuscript; available in PMC 2016 January 09.

Published in final edited form as:

IEEE Trans Neural Syst Rehabil Eng. 2012 November ; 20(6): 853–857. doi:10.1109/TNSRE.2012.2184769

Towards a Healthy Human Model of Neural Disorders of Movement

Howard Poizner,
Institute for Neural Computation, University of California-San Diego, La Jolla, CA 92093 USA and also with the Graduate Program in Neurosciences, University of California-San Diego, La Jolla, CA 92093 USA

Jack Lancaster,
Research Imaging Institute, University of Texas Health Science Center, San Antonio, TX 78285 USA

Eugene Tunik,
Department of Rehabilitation and Movement Science, University of Medicine and Dentistry of New Jersey, Newark, NJ 07107 USA

Shalini Narayana,
Research Imaging Institute, University of Texas Health Science Center, San Antonio, TX 78285 USA

Crystal Franklin,
Research Imaging Institute, University of Texas Health Science Center, San Antonio, TX 78285 USA

William Rogers,
Research Imaging Institute, University of Texas Health Science Center, San Antonio, TX 78285 USA

Xiaoyan Li,
Institute for Neural Computation, University of California-San Diego, La Jolla, CA 92093 USA

Peter T. Fox, and
Departments of Neurology and Radiology, and Program in Biomedical Engineering, University of Texas Health Science Center, San Antonio, TX 78285 USA, and also with the Research Imaging Institute, University of Texas Health Science Center, San Antonio, TX 78285 USA

Donald A. Robin
Honors College, University of Texas, San Antonio, TX 78249 USA, and also with Departments of Neurology and Radiology, and Program in Biomedical Engineering, University of Texas Health Science Center, San Antonio, TX 78285 USA, and also with Research Imaging Institute, University of Texas Health Science Center, San Antonio, TX 78285 USA

Abstract

A quantitative approach to virtual-lesion physiology is presented which integrates event-related fMRI, image-guided, repetitive, transcranial magnetic stimulation (irTMS), and simultaneous recording of 3-D movement kinematics. By linking motor neuroscience with clinical disorders of

motor function, our method allows development of a healthy, human system model of disorders of skilled action.

Keywords

Apraxia; brain imaging; kinematics; motor control

I. Introduction

Investigations of neural disorders of skilled movement traditionally have studied the effects of naturally occurring lesions, which tend to be widespread [1]. The present paper provides a complementary approach by creating a healthy human system model of such disorders. We present a proof-of-principle demonstration, taking as a test case limb apraxia, an inability to imitate or perform skilled object-related actions appropriately despite the absence of gross weakness, sensory loss or incoordination [2]. We first use functional magnetic resonance imaging (fMRI) to examine those neural systems that are activated in normal subjects when producing a key gesture previously studied in apraxic patients, that of slicing of an object, such as a loaf of bread.

We expect brain networks to be activated that support such skilled object-related action. After identifying regions involved in the slicing gesture, we use the fMRI maps to guide subject-specific neuronavigation with robotically positioned, repetitive transcanial magnetic stimulation (irTMS) [3]. Finally, we deliver irTMS during movement (peri-movement) to directly test the causal involvement of these regions in gestural production. Peri-movement irTMS provides an ideal platform for testing the causal role of brain regions identified with fMRI, because, utilizing 3-D motion capture, we can quantify kinematic performance in stimulation-on and off (control) conditions and, by temporarily disrupting activity in a given region, bring to bear the only tool that can by used to attribute anatomic-functional causality in healthy humans. In what follows, we describe this new integration of fMRI, irTMS and 3-D motion capture, providing a quantitative approach to virtual-lesion physiology.

II. Methods

Subjects

Seven healthy, right-handed volunteers participated (Experiment 1, $n = 7$, 5 males mean age ±1 standard deviation [SD]: 45.6 ± 12.4 years; Experiment 2, $n = 3$, 2 males, 51.3 ± 14.6 years). The subjects in Experiment 2 also participated in Experiment 1. Handedness was self-reported. Seven faculty members and postdoctoral fellows (four co-authors, three nonauthors) served as subjects for this pilot study. No participant had any metal or medication contraindication for participating in fMRI and TMS studies. The study was done in advance of getting IRB approval, but included only investigators. At the University of Texas Health Science Center, San Antonio, investigator self-study is accepted as not requiring signed informed consent, as investigators are well informed about potential study risks.

A. General Experimental Setup

Imaging—MRI scanning was carried out on a 3T Siemens Trio system in the Research Imaging Center, UTHSCSA. Procedures for BOLD fMRI data acquisition, anatomical image preprocessing, and functional image preprocessing have been previously described [4]–[8]. *Combined irTMS and 3-D motion capture*. Fig. 1 illustrates the experimental setup. A five degree-of-freedom neurosurgical robotic system (NeuroMate, ISS, Paris, France) was adapted to precisely aim and hold the TMS coil over the brain area to be stimulated. The system's overall accuracy in positioning the planned site of the TMS coil is exceptional, ~2 mm [3], [9]. TMS was applied using a water-cooled Cadwell Fig. 8 coil (Cadwell, Inc., Kennewick, WA; see [10] for a description of the Cadwell coil's E-field). 3-D motion capture was performed using a two-beam Optotrak Certus 3-D tracking system (Northern Digital, Inc., Waterloo, ON, Canada). Infrared emitting diodes were taped to the right cheek, the major joints of the arm, the dorsal surface of the palm, and the right hip. 3-D marker positions were recorded at 200 Hz.

B. General Experimental Procedure

Behavioral Tasks—Subjects were asked to perform two tasks: 1) right index finger tapping and 2) pantomime the slicing of bread, without shoulder movement, using the right arm. The slicing gesture was similar to the one we have previously used [11]–[13]. The finger tapping and the slicing gesture were self-paced at 1 Hz to minimize rate-related confounds on the fMRI blood oxygen level-dependent (BOLD) signal or cortical stimulation. Subjects practiced the tasks before the fMRI session to ensure that they could reproduce the gesture at 1 Hz, and then practiced again inside the fMRI scanner (immediately before data collection) to ensure that the correct rate was kept constant while head movement was kept to a minimum. Additionally, the participants practiced the slicing task prior to the irTMS session. A camera recording in the MRI suite allowed for viewing subjects to ensure that movements were produced at 1 Hz.

Experiment 1—Experiment 1 was a blocked-design fMRI experiment to identify neural substrates recruited during repetitive slicing gestures and tapping movements. These data were used for neuronavigation of TMS loci in Experiment 2. Subjects performed the slicing emulation for 30 s epochs followed by 30 s of rest, for a total of four runs of task and rest, collected during 4 min of scan. In separate scan, subjects performed the finger tapping task at 1 Hz, also in block design (30 s task and 30 s of rest for a total of 4 min). Thus, we could compare brain activation involved in slicing with that of another type of repeated movement within the limb motor system.

Experiment 2—Experiment 2 was a within subjects, irTMS-on and irTMS-off, design. A virtual lesion model induced by peri-movement irTMS was used to test the causal anatomic-functional relationship between three regions identified in Experiment 1. We predicted that temporary disruption of activity in regions which are causally involved in slicing gestures (identified in Experiment 1) should reflect as impoverished spatiotemporal kinematic profiles.

Imaging Analysis—Within-subject statistical images were created by contrasting each movement condition (slicing and tapping) with rest. For group analysis, individual images were aligned to the respective anatomical images that were previously normalized into a standard stereotactic space [6]. These activation maps were thresholded based on magnitude and extent of activation [7], [8], and controlled for multiple comparisons using Bonferroni correction. In addition, regions of interest (ROI) were used in subsequent data analysis. The group contrasts of slicing > rest and tapping > rest were submitted to ANOVA. Subtracting a common rest baseline from each discrete task condition assures that activation reflects differences in task rather than baseline state. Activation volumes with $p < 0.05$ (after correction for multiple comparisons) are reported.

Neuro-Navigation—The individual conditional contrasts of the finger tapping and slicing tasks were registered to their respective anatomical MRI (aMRI). Prior to study day, target sites such as left primary motor cortex arm area (M1), supplementary motor area (SMA), and posterior parietal cortex (PPC) were identified from the slicing task contrasted with rest. The average location for M1 in Talairach coordinates (x, y, z) was −33, −28, 54; for SMA was −8, −29, 54; and PPC was −43, −50, 43. Positioning the coil was planned for each site individually for each participant, from the individual 3-D images. On the day of the study, the insitu head position was registered to its anatomical MRI image; the robot's coordinate system was registered to the insitu head; and the TMS coil was robotically positioned to the planned pose. Motor threshold was determined as the lowest intensity of TMS that resulted in motor evoked potentials of 100μV amplitude in 5 out of 10 trials when TMS was applied to M1. Each epoch of irTMS consisted of 5 s of 4 Hz TMS applied at 125%–130% of motor threshold followed by 5 s of no irTMS. Six such epochs were delivered at each location (1 min). During no irTMS conditions, the TMS coil was still positioned at the location, but the TMS unit was not discharged. The order of stimulation sites was counterbalanced across subjects. The irTMS on and off blocks were run consecutively with subjects continually making the movement throughout the interval (60 s). TMS parameters (rate, intensity, and duration) were within the safety guidelines [14], [15].

Kinematic Outcome Measures—Spatiotemporal patterns inherent in the digital records of the limb trajectories were quantified using the following measures: *Linearity* and *planarity* of the hand trajectories (higher scores reflect more linear and planar movements, respectively) [6]–[8], and normalized integrated jerk (NIJ; [16] (lower scores reflect smoother hand velocity profiles). Detailed descriptions of these measures can be found at [11], [12], and [17].

Statistical Analysis—Due to the small sample size, statistical comparisons were performed at the single-subject level (within subjects) using nonparametric statistics (Mann–Whitney U Test). The following pair-wise comparisons were performed: To examine the role of specific cortical regions on performance, we compared the irTMS-on and irTMS-off conditions, when irTMS was delivered to PPC, SMA, and M1 arm regions on performance. The analyses were carried out separately for each dependent measure of linearity, planarity, and NIJ for each subject. To reduce chances of Type I error due to multiple comparisons, alpha was set to 0.008 (0.05/6).

III. Results

Experiment 1

Contrastive fMRI results (TASK-REST) of areas active during slicing and finger tapping are shown in Tables I and II. Only regions that reached statistical significance are shown in the Tables. Fig. 2(A) shows regions significantly activated in the slicing-rest contrast. The areas of peak activations for slicing were localized to the hand and shoulder representations of the left M1 (BA4), the left superior and inferior parietal lobe (BA 2, 3; including the hand–shoulder areas of the somatosensory cortex, (S1), and the left SMA. Conversely, finger tapping activated a broader network of bilateral cortical regions and subcortical structures than did slicing [see Table II and Fig. 2(B)]. Regions involved in finger tapping included the hand representation of left M1 (BA4), right cingulate (BA32), left pre-motor cortex (BA6), left and right insula (BA 13), left pulvinar, left temporal lobe (BA22, 41, 42), and cerebellum. Finger tapping did not elicit parietal activations.

Experiment 2

Fig. 3(A) displays the 3-D hand path of a typical subject (J) who performed cycles of slicing gesture during the irTMS-on (left panels) and irTMS-off (right panels) conditions. When irTMS was off, the hand travelled consistently in the sagittal plane in a highly linear path (Fig. 3(A), right panels). Sharp reversals were observed between the forward and backward strokes. In addition, tangential velocities showed sinusoidal variations (Fig. 3(A), inset). Conversely, Fig. 3(A) (left panels) illustrates that when irTMS was applied to the parietal and M1 sites, the spatiotemporal profiles of the hand trajectory considerably deteriorated. Specifically, subjects exhibited larger excursions in the lateral direction, nonlinear and nonplanar trajectories, and blunted stroke reversals. Moreover, the tangential velocity profile was less sinusoidal and more variable than that of the irTMS-off condition. Importantly, irTMS to SMA did not produce such performance decrements Fig. 3(A), middle panel), suggesting that the effects were localized to the parietal and M1 sites.

Fig. 3(B) shows the mean (±1 SD) linearity, planarity, and NIJ indices for each subject's hand path in the irTMS-on and irTMS-off conditions, for each stimulation site. No significant differences were found between the irTMS-on and irTMS-off conditions for linearity, planarity, and NIJ for the SMA site. However, there were significant decreases in linearity and planarity, and increases in NIJ while irTMS was applied to the other two sites. Specifically, statistical analysis revealed a consistent main effect of irTMS for linearity [top panel of the Fig. 3(B)] when the irTMS was applied to parietal cortex ($p < 0.002$ for all subjects). Fig. 3(B) (middle) also shows that there was a main effect of irTMS for planarity across for the parietal site ($p < 0.0005$ for all subjects). Finally, Fig. 3(B) (bottom) shows a main effect of irTMS for NIJ for the parietal ($p < 0.005$ for all subject) and M1 sites ($p < 0.0001$ for subjects J and B).

IV. Discussion

We combined event-related fMRI, lesion modeling using irTMS, and analysis of 3-D movement kinematics to show that the relatively well-learned gesture emulating slicing

recruits a motor-SMA-parietal network and that transient peri-movement disruption of the M1 and parietal sites leads to immediate and notable decrements in trajectory control characteristic of the impairments observed in apraxic patients [12], [18]. It is noteworthy that irTMS of a nonmotor area of the cortex (PPC) as well as of M1, but not of an adjacent premotor area (SMA) elicited the uncoordinated movement patterns, suggesting that the effects were highly region-specific.

Our findings confirm previous reports showing that disruption of M1 produces deficits in accuracy and timing of sequential motor tasks [19]. We did observe an ~4 Hz oscillation ("twitching") in the hand trajectory during M1 stimulation, and to some extent during parietal stimulation. This could have explained some of the disruption observed at M1. However, as shown in Fig. 3(A), disruptions following M1 stimulation differed markedly from those following parietal stimulation, consistent with subjects' reports of "I know what I want to do but I can't control my hand," following parietal stimulation. It has been recently demonstrated that transient (using single or triple) TMS pulses delivered to adjacent regions of the parietal lobe either during a memory interval preceding a reaching and saccadic movement [20] or during adaptation to novel reaching/grasping demands [21], [22] also leads to decrements in accuracy. That work has highlighted the potential causal role of the parietal cortex in online adaptation to reconcile movement errors. Our findings, that peri-movement irTMS disrupts spatiotemporal aspects of movement trajectories for the duration of the stimulation epoch, irrespective of the need to adapt, are a strong indicator that PPC may not only be performing critical online computations during visually-guided tasks, but may also be critically involved in the read-out of memory traces of learned, skilled gestures.

In recent years it has become clear that sensory systems and motor systems are inseparably intertwined. For example, patients with loss of proprioception, but with motor fibers intact, show marked impairments in the control of multi-joint movements [11], [23]. Indeed, patients with this sensory loss, as well as patients with apraxia, exhibit distortions in trajectory linearity, planarity, and velocity smoothness when producing the slice gesture [11]. Given the close proximity of somatosensory cortex and the PPC, and given that both of these regions were activated during fMRI in Experiment 1, we cannot rule out the possibility that our irTMS stimulation disrupted proprioceptive processing, which in turn may have contributed to the observed movement abnormalities. Clearly larger studies will be needed to confirm and extend these findings. However, the present report provides a proof-of-principle that integrating fMRI, irTMS, and 3-D motion capture is a promising avenue for linking motor neuroscience with clinical disorders of motor function, and that it may allow development of a healthy system model for studying apraxia and other neural disorders of movement.

Acknowledgment

The authors would like to thank A. E. Ramage, A. Jacks, P. Kochunov, and D. Lee for their help, and thank Cerebral Magnetics, LLC for technical support of the irTMS system. P. Fox and J. Lancaster are principles in Cerebral Magnetics, which holds IP for irTMS and the cortical column cosine TMS aiming strategy.

The work of S. Narayana was supported by R21 DC009467. The work of S. L and D. Robin was supported by R01 DC006243. The work of H. Poizner was supported in part by ONR MURI under Award N00014-10-1-0072 and in part by the National Institutes of Health (NIH) under Grant 2 R01 NS036449. The work of E. Tunik was supported

by the NIH under grant K01 HD059983. This work was also supported by the National Science Foundation (NSF) under Grant ENG-1137279 (EFRI M3C) and Grant SBE-0542013 to the Temporal Dynamics of Learning Center, an NSF Science of Learning Center.

REFERENCES

1. Lomber SG. The advantages and limitations of permanent or reversible deactivation techniques in the assessment of neural function. J. Neurosci. Methods. 1999 Jan.86(2):109–117. [PubMed: 10065980]
2. Heilman, KM.; Valenstein, E., editors. Clinical Neuropsychology. 4th. Oxford, U.K.: Oxford Univ. Press; 2003.
3. Lancaster JL, Narayana S, Wenzel D, Luckemeyer J, Roby J, Fox P. Evaluation of an image-guided, robotically positioned transcranial magnetic stimulation system. Human Brain Mapp. 2004 Aug. 22(4):329–340.
4. Kochunov P, et al. Retrospective motion correction protocol for high-resolution anatomical MRI. Human Brain Mapp. 2006 Dec.27(12):957–962.
5. Jenkinson M, Bannister P, Brady M, Smith S. Improved optimization for the robust and accurate linear registration and motion correction of brain images. NeuroImage. 2002 Oct.17(2):825–841. [PubMed: 12377157]
6. Bullmore E, et al. Statistical methods of estimation and inference for functional MR image analysis. Magn. Reson. Med. 1996 Feb.35(2):261–277. [PubMed: 8622592]
7. Sidtis JJ. Some problems for representations of brain organization based on activation in functional imaging. Brain Language. 2007 Aug.102(2):130–140. [PubMed: 16938343]
8. Woolrich MW, Ripley BD, Brady M, Smith SM. Temporal autocorrelation in univariate linear modeling of FMRI data. NeuroImage. 2001 Dec.14(6):1370–1386. [PubMed: 11707093]
9. Epstein CM, Schwartzberg DG, Davey KR, Sudderth DB. Localizing the site of magnetic brain stimulation in humans. Neurology. 1990 Apr.40(4):666–670. [PubMed: 2320243]
10. Salinas FS, Lancaster JL, Fox PT. 3-D modeling of the total electric field induced by transcranial magnetic stimulation using the boundary element method. Phys. Med. Biol. 2009 Jun; 54(12): 3631–3647. [PubMed: 19458407]
11. Sainburg RL, Poizner H, Ghez C. Loss of proprioception produces deficits in interjoint coordination. J. Neurophysiol. 1993; 70(5):2136–2147. [PubMed: 8294975]
12. Clark MA, et al. Spatial planning deficits in limb apraxia. Brain. 1994 Oct.117(5):1093–1106. [PubMed: 7953591]
13. Poizner H, Clark MA, Merians AS, Macauley B, Rothi LJG, Heilman KM. Joint coordination deficits in limb apraxia. Brain. 1995 Feb.118:227–242. [PubMed: 7895006]
14. Wassermann EM. Risk and safety of repetitive transcranial magnetic stimulation: Report and suggested guidelines from the international workshop on the safety of repetitive transcranial magnetic stimulation, June 5–7, 1996. Electroencephalogr. Clin. Neurophysiol. 1998 Jan.108(1): 1–16. [PubMed: 9474057]
15. Rossi S, Hallett M, Rossini PM, Pascual-Leone A. Safety, ethical considerations, and application guidelines for the use of transcranial magnetic stimulation in clinical practice and research. Clin. Neurophysiol. 2009 Dec.120(12):2008–2039. [PubMed: 19833552]
16. Tresilian J, Stelmach GE, Adler CH. Stability of reach-to-grasp movement patterns in Parkinson's disease. Brain. 1997 Nov.120(11):2093–2111. [PubMed: 9397024]
17. Poizner H, et al. The timing of arm-trunk coordination is deficient and vision-dependent in Parkinson's patients during reaching movements. Exp. Brain Res. 2000 Aug.133:279–292. [PubMed: 10958518]
18. Poizner H, Mack L, Verfaellie M, Rothi LJ, Heilman KM. Three-dimensional computergraphic analysis of apraxia. Neural representations of learned movement. Brain. 1990 Feb.113:85–101. [PubMed: 2302539]
19. Gerloff C, Corwell B, Chen R, Hallett M, Cohen LG. Stimulation over the human supplementary motor area interferes with the organization of future elements in complex motor sequences. Brain. 1997 Sep.120(9):1587–1602. [PubMed: 9313642]

20. Vesia M, Prime SL, Yan X, Sergio LE, Crawford JD. Specificity of human parietal saccade and reach regions during transcranial magnetic stimulation. J. Neurosci. 2010 Sept.30(39):13053–13065. [PubMed: 20881123]
21. Della-Maggiore V, Malfait N, Ostry DJ, Paus T. Stimulation of the posterior parietal cortex interferes with arm trajectory adjustments during the learning of new dynamics. J. Neurosci. 2004 Nov.24(44):9971–9976. [PubMed: 15525782]
22. Tunik E, Frey SH, Grafton ST. Virtual lesions of the anterior intraparietal area disrupt goal-dependent on-line adjustments of grasp. Nature Neurosci. 2005 Apr.8(4):505–511. [PubMed: 15778711]
23. Sainburg RL, Ghilardi MF, Poizner H, Ghez C. Control of limb dynamics in normal subjects and patients without proprioception. J. Neurophysiol. 1995; 73(2):820–835. [PubMed: 7760137]

Biographies

Howard Poizner is a Research Professor in the Institute of Neural Computation, and a member of the Program in Neurosciences at the University of California, San Diego. His research interests involve the neural control of movement.

Prof. Poizner is the 2002 recipient of the Rutgers University Board of Trustees Excellence in Research Award.

Jack Lancaster is Professor of Radiology at the University of Texas Health Science Center at San Antonio (UTHSCSA). He is the Associate Director of the Research Imaging Institute (RII) and Chief of the RII's Biomedical Image Analysis Division. He is also Chair of the Imaging track for the joint Biomedical Engineering Program at UT San Antonio and UTHSCSA. His primary research interests are transcranial magnetic stimulation and medical image processing.

Crystal Franklin is a Statistician-Intermediate in the Research Imaging Institute at University of Texas Health Science Center at San Antonio. Her research interests involve learning new techniques and software used for analyzing fMRI, PET, and clinical data.

Xiaoyan Li was a Postdoctoral Research Fellow in Institute for Neural Computation of the University of California at San Diego. Currently she is a Research Associate at the Sensory Motor Performance Program of the Rehabilitation Institute of Chicago, IL. Her research interests focus on motor control, neurological disorders and rehabilitation.

Peter Fox is the current and founding Director of the Research Imaging Center at University of Texas Health Science Center at San Antonio, where he also is Professor of Radiology, Neurology, Psychiatry and Physiology. His research interests involve advancing the scientific discipline of imaging-based neuroscience.

Prof. Fox is a fellow of the American Association for the Advancement of Science.

Donald Robin is Professor and Division Chief, Human Performance Division and Assistant Co-Director for Education at the Research Imaging Center at UTHSCSA, and Professor, Departments of Neurology, Radiology, and Biomedical Engineering at University of Texas Health Science Center at San Antonio. He also is Professor, Honors College, University of Texas, San Antonio. His research interests involve the study of the neural substrates of speech and limb motor control.

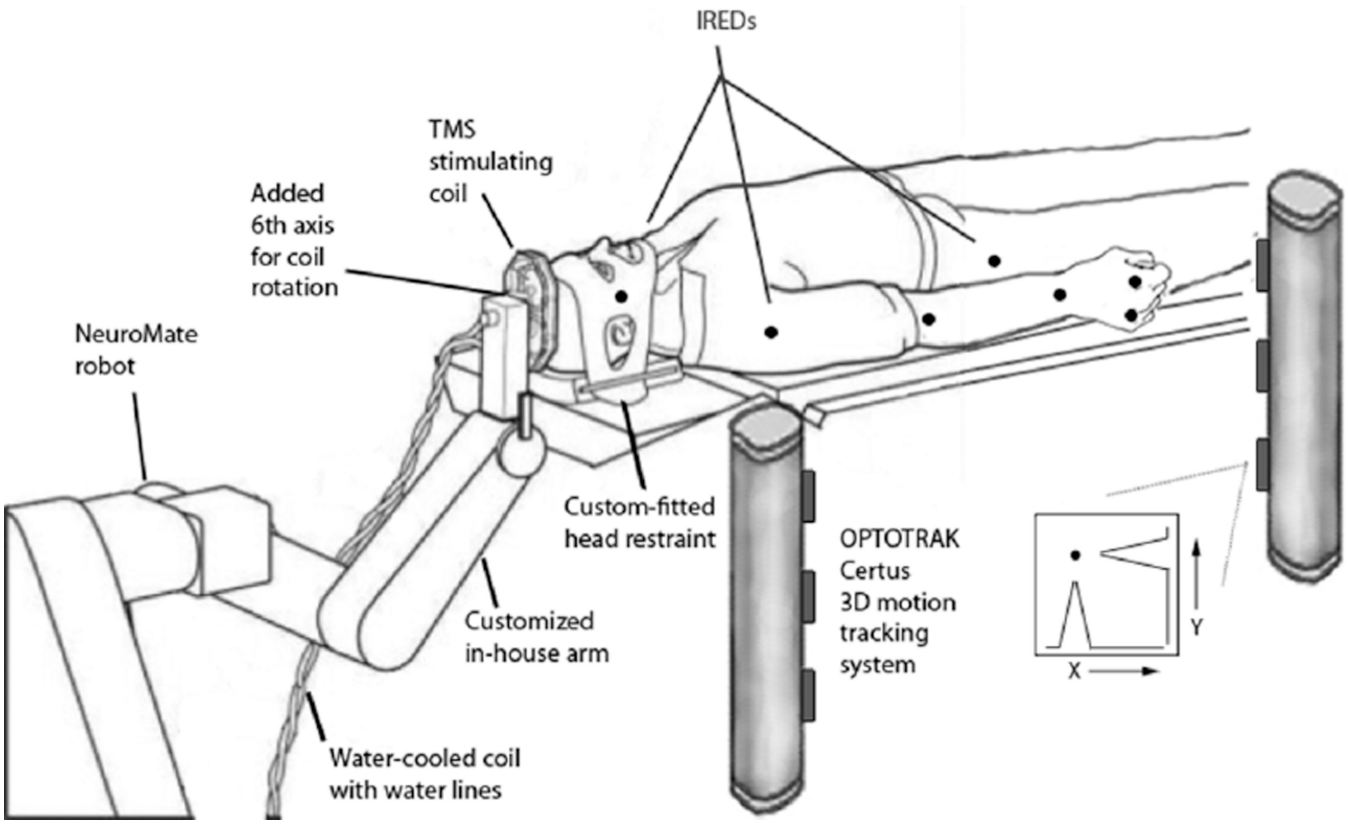

Fig. 1.

Experimental setup for combined irTMS and 3-D motion capture. A customized neurosurgical robotic system (NeuroMate, ISS, Paris, France) was used to precisely position the TMS coil. A 2-beam Optotrak Certus (Northern Digital, Inc.) 3-D motion tracking system was used to monitor all movements.

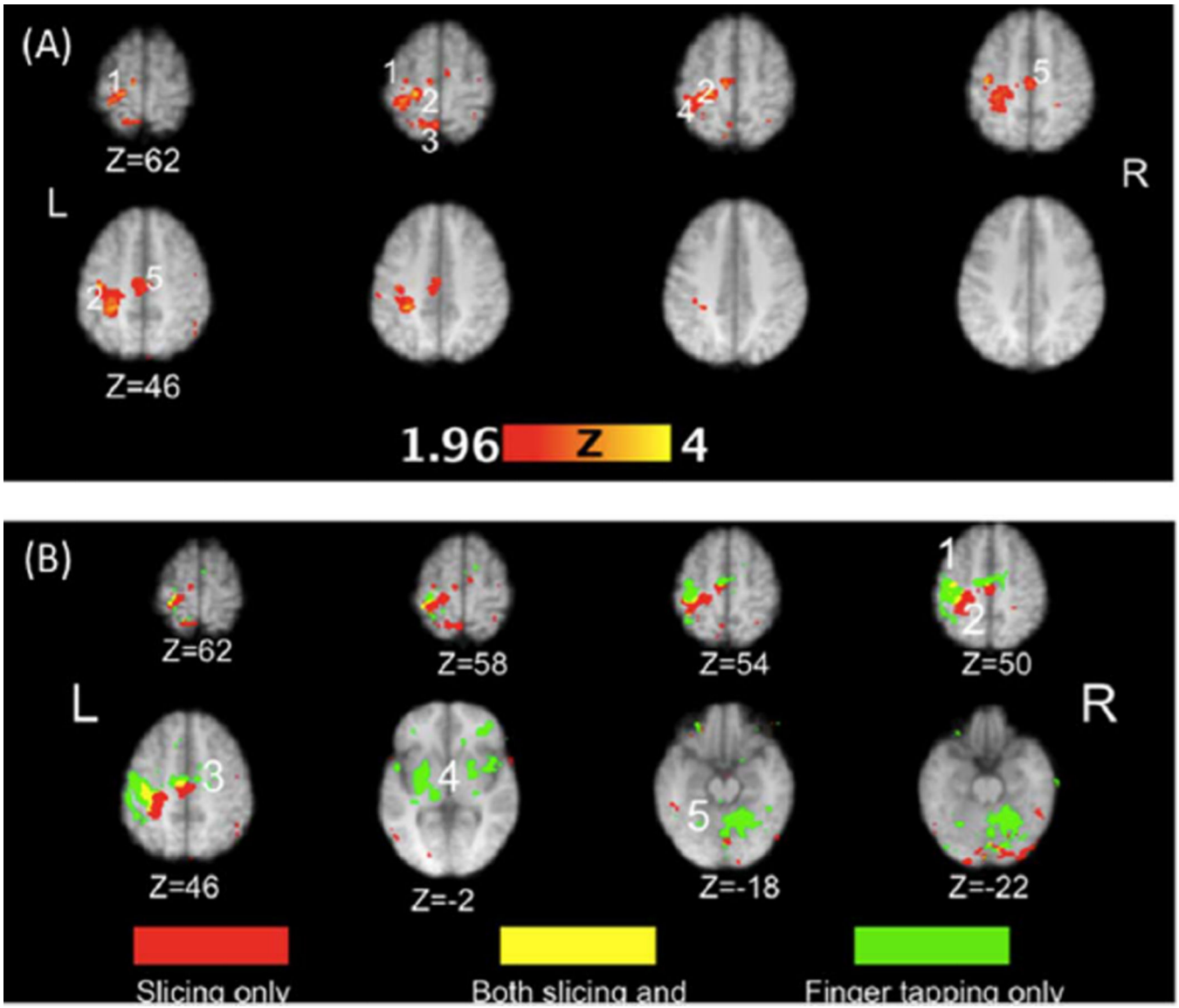

Fig. 2.

(A). Regions significantly activated in the slicing condition at the group level. The numbers denote functional or anatomical localizers for the hand area of primary motor (1) and somatosensory (2) cortex, superior (3) and inferior (4) parietal lobule, and supplementary motor area (5). (B). Significant activation related exclusively to the slicing only (red) and finger tapping only (green) conditions. A conjunction analysis (yellow) shows regions significantly activated in both conditions. The numbers denote functional or anatomical localizers for the hand area of primary motor (1) and somatosensory (2) cortex, supplementary motor area (3), basal ganglia and thalamus (4), and cerebellum (5).

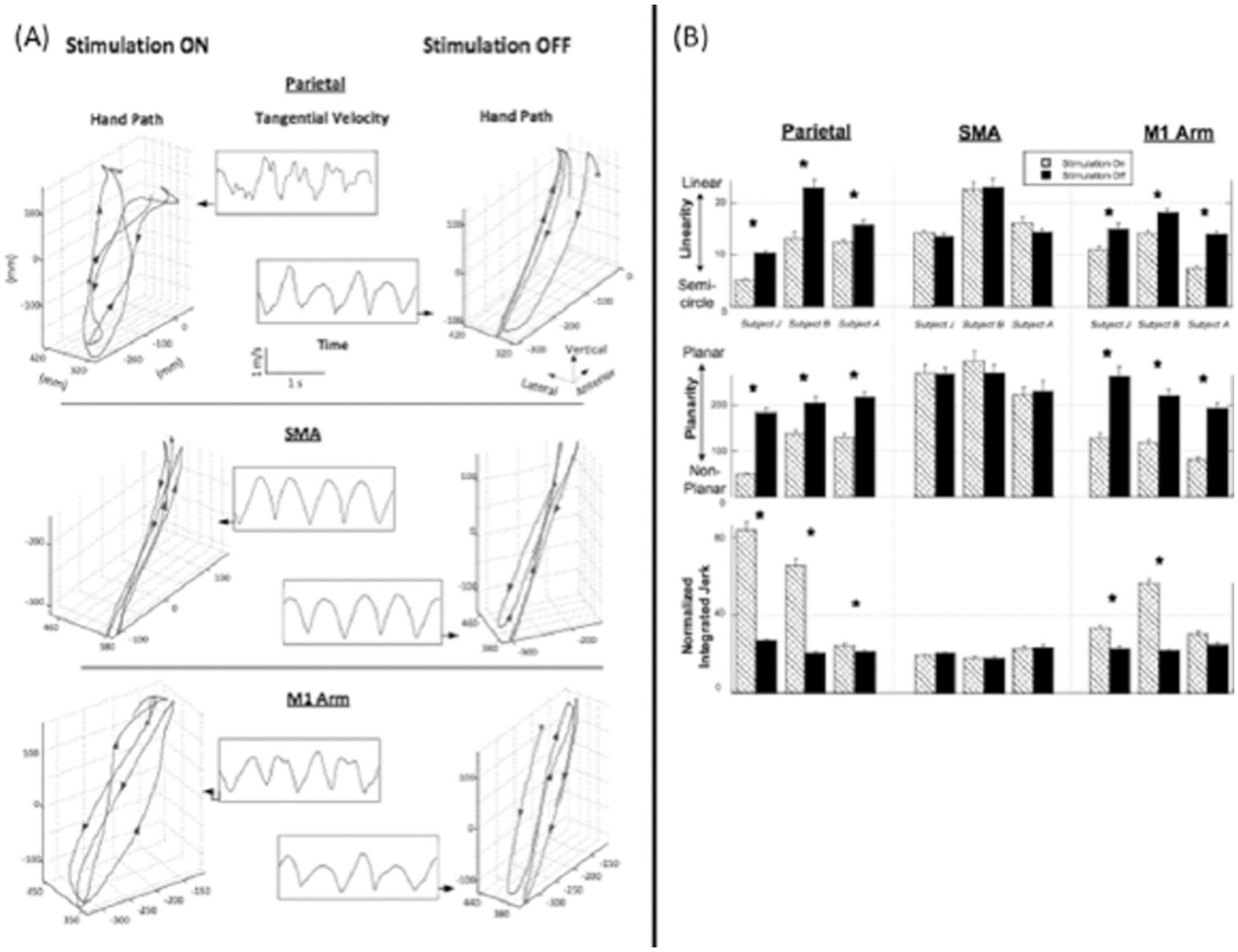

Fig. 3.

(A) Hand paths for one typical subject, plotted in 3-D space, for the TMS-on (left panels) and TMS-off (right panels) epochs. The tangential velocities, plotted as a function of time, are shown for each respective condition in the middle panels. Data for stimulation over parietal, supplementary motor area, and motor cortex regions are shown in the top, middle, and lower panels, respectively. Note the marked disruption in the spatiotemporal profiles elicited by parietal and motor stimulation, but not by supplementary motor area stimulation. (B) Kinematic indices of task performance shown at the single subject level (±1 SD) for the trajectory linearity, planarity, and movement smoothness (NIJ) during irTMS ON and OFF epochs over left parietal, SMA, and M1 cortical regions. Asterisks denote significant differences between the TMS-on and TMS-off conditions.

TABLE I

Coordinates of Activation During Slicing Versus Rest

Lobe	region (Brodmann area)	X	Y	Z	Z scare
Frontal lobe	left M1-shoulder (BA4)	−18	−30	64	3.77
	left M1-hand (BA 4)	−38	−20	52	4.00
	SMA				
Parietal lobe	left S1 (BA 2)	−30	−36	62	3.5
	left S1 (BA 3)	−22	−30	60	4.26
	left superior parietal lobule (BA 5)	−34	−42	60	2.93
	left S1(BA 3)	−38	−20	48	3.91
	left S1(BA 3)	−28	−38	44	3.54
	left precuneus				
	left inferior parietal lobule				

TABLE II

Coordinates of Activation During Finger Tapping Versus Rest

Lobe	region (Brodmann area)	X	Y	Z	Z score
Frontal lobe	left M1-hand (BA 4)	−40	−20	54	3.70
	SMA				
	right cingulate (BA 32)	18	20	28	3.03
	right cingulate (BA 32)	22	18	26	2.97
	left Pmd (BA 6)	−48	−2	6	3.50
sublobar regions	left Insula (BA 13)	−42	−38	18	3.33
	right Insula (BA 13)	42	−2	8	2.90
subcortical regions	left pulvinar	−16	−26	6	3.28
	left Putamen	−26	−4	2	3.37
temporal lobe	left BA 22	−48	0	2	3.40
	left BA 41	−46	−28	18	3.77
	left BA 42	−54	−32	14	3.31
cerebellum	right cerebellum (dentate)	14	−60	−26	3.02